The International Journal of Advanced Manufacturing Technology (2023) 124:4349–4363
https://doi.org/10.1007/s00170-022-09617-y

ORIGINAL ARTICLE

Accuracy decay mechanism of ball screw in CNC machine tools for mixed sliding-rolling motion under non-constant operating conditions

Baobao Qi[1,2] · Jiajia Zhao[3] · Chuanhai Chen[1,2] · Xianchun Song[3] · Hongkui Jiang[3]

Received: 5 May 2022 / Accepted: 25 June 2022 / Published online: 12 July 2022

Abstract
The ball screw (BS) has become an indispensable key functional component in many fields, such as CNC machine tools, precision transmission system, and special service requirements. Its accuracy reliability is a key performance in many application fields. There is a phenomenon of mixed slip-roll motion during the BS operation; however, both non-constant working conditions and mixed sliding-rolling motion mode affect its accuracy decay. In this paper, the modeling method of accuracy decay for mixed sliding-rolling motion behavior is established under non-constant operating conditions. The accuracy reliability of the BS is analyzed under single non-constant operation condition or multiple non-constant operating conditions, and the accuracy decay is predicted though modeling method proposed. In addition, the experimental analysis of the BS accuracy degradation is carried out under three different amplitudes of AL (non-constant axial load), FR (non-constant feed rate), and AL + FR combination conditions. The average value of the accuracy loss relative error (5.90 ~ 8.50%) between theoretical model and experimental test results is smaller than that (11.18 ~ 12.66%) under pure sliding motion. It shows that the accuracy decay analysis model established is beneficial to predict the BS accuracy reliability.

Keywords Ball screw · Accuracy decay · Experimental analysis · Non-constant operating condition · Mixed sliding-rolling motion

1 Introduction

The research on the BS accuracy degradation in CNC machine tools was mainly carried out through wear modeling and degradation analysis. The analysis of mechanics and kinematics is basis for the research on the accuracy decay mechanism of the BS. According to mechanics and kinematics of BS [1–3], the relative motions between the ball and the raceway include rolling and sliding [4, 5].

As a functional component of CNC machine tools, considering the sliding motion mode between the ball and the raceway, the accuracy decay modeling, accuracy decay test, and prediction analysis were carried out. The Archard model [6] was commonly used in the field of BS wear. Wei [7] and Xu [8] et al. established the BS wear model based on modified Archard model. Xu et al. [9] predicted the BS accuracy decay value according to the wear behavior analysis. Zhou et al. [10] introduced the parameter K' to correct the main wear area, in order to study the relationship between feed rate, high load conditions, and wear rate. After that, Zhou et al. [11] improved the wear coefficient of the ball screw through combining theoretical analysis and experimental test. However, Luo and Dornfeld [12] and Horng [13] established the two-body microscopic wear model based on micro-contact theory, in order to explain the relationship between the wear depth and the actual feed stroke. Zhao et al. [14, 15] took the double-nut preloaded ball screw as the research object and successively studied the wear

✉ Jiajia Zhao
zhaojiajia21@sdjzu.edu.cn

✉ Chuanhai Chen
cchchina@foxmail.com

[1] Key Laboratory of CNC Equipment Reliability, Ministry of Education, Changchun 130022, Jilin Province, China

[2] School of Mechanical and Aerospace Engineering, Jilin University, Changchun 130022, Jilin Province, China

[3] School of Mechanical and Electrical Engineering, Shandong Jianzhu University, Jinnan 250101, Shandong Province, China

behavior through modeling and experimental verification. According to the research basis [7, 9, 10], Liu et al. [16] introduced fractal theory into wear modeling to study the accuracy degradation mechanism of the BS. And the model proposed was compared with the Wei et al. [7] model from the perspective of prediction accuracy. Wang et al. [17] studied the raceway profile for the BS, indicating that measuring basis is an influence factor of the raceway error on positioning precision. Zhao et al. [18] studied the accuracy degradation behavior of double-nut ball screws due to raceway wear based on fractal theory [16].

When considering the mixed sliding-rolling motion between the ball and the raceway in CNC machine tools, the research on the accuracy degradation of the BS was still in the preliminary stage. Rolling motion analysis of BS was usually combined with creep theory [19, 20]. Then, Xu et al. [20] established a friction force model of the BS based on creep theory. Qi et al. [21] studied the accuracy decay law of the BS through the mixed sliding-rolling motion analysis, but did not consider the time-varying operating conditions. In addition, Cheng et al. [22, 23] carried out accuracy decay prediction and life prediction research according to wear analysis, respectively. In contrast, considering the plastic deformation and random distribution characteristics of rough contact surface, Pullen and Williamson [24] and Williamson and Harris [25] established PW model of wear failure based on random factors. Cheng et al. [26] and Hu et al. [27] studied the ball screw accuracy loss characteristics caused by sliding motion under time-varying axial loads and feed rates. Zhang et al. [28], Niu et al. [29], and Jin et al. [30] studied the machining quality evaluation and machining accuracy improvement of multi-axis CNC machine tools, through analyzing the geometric errors of key functional components. When considering economic dependence and structural dependence, Sun et al. [31] established the group maintenance strategy of CNC machine tools. Aiming at the influence of geometric error for CNC machine tools, Guo et al. [32] introduced the global quantitative sensitivity method to analyze error compensation. Based on the measured geometric error parameters, Wu et al. [33] and Niu et al. [34] analyzed the machining accuracy reliability of CNC machine tools combining with the response surface method. In addition, Zhang et al. [35] proposed a rapid construction method of equipment model for a discrete manufacturing.

Despite the progress, the operating conditions of the BS have non-constant characteristics in CNC machine tools, and the accuracy degradation and experimental research are still in the preliminary stage under non-constant operating conditions. The influences of non-constant operating conditions and mixed sliding-rolling motion mode on accuracy decay behavior of BS have rarely been studied. And the accuracy reliability analysis and experimental study of BS for mixed sliding-rolling motion has also rarely been studied under non-constant operating conditions. To solve these problems, the accuracy decay modeling of the BS was established under the sliding motion or rolling motion behavior, respectively. And the mechanism analysis of the accuracy decay was studied considering the mixed sliding-rolling motion mode. Furthermore, an experimental study on the BS accuracy degradation was carried out considering the non-constant operating conditions.

2 Modeling of accuracy decay for mixed sliding-rolling motion

2.1 Accuracy decay modeling for sliding motion under non-constant conditions

In a certain type of machine tool, due to the change of external load conditions, the loading states of the left and right nuts are different, as shown in Fig. 1.

According to Fig. 1, the accuracy decay of the double-nut BS is required to analyze the cumulative wear between the left/right nut and the screw separately, then:

$$\begin{aligned} V(t) &= V_{b-s}(t) + V_{b-n}(t) \\ &= K_{b-s}\frac{Q_{b-s}(t)S_{b-s}(t)}{H_{b-s}} + K_{b-n}\frac{Q_{b-n}(t)S_{b-n}(t)}{H_{b-n}} \end{aligned} \tag{1}$$

Among them, $V_{b-s}(t)/V_{b-n}(t)$ represents the real-time wear amount between the ball and the screw/nut raceway, respectively. $Q_{b-s}(t)$ / $Q_{b-n}(t)$ is the contact load between the ball and the screw/nut raceway at time t.

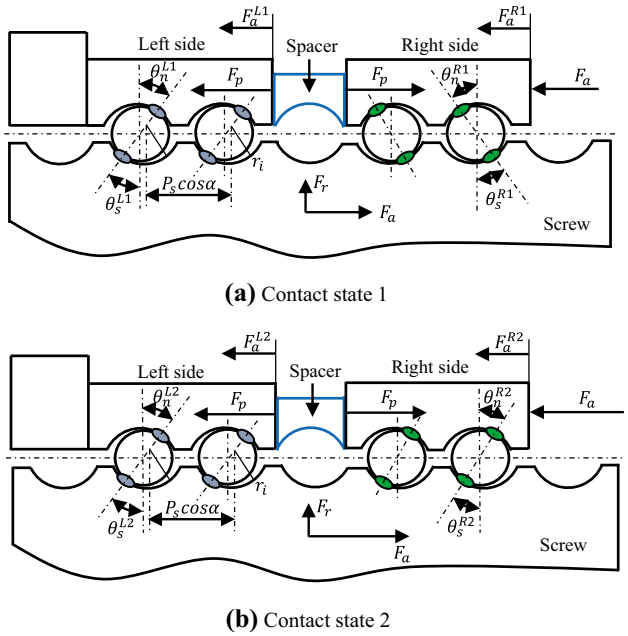

(a) Contact state 1

(b) Contact state 2

Fig. 1 Ball screw loading state. **a** Contact state 1. **b** Contact state 2

If the BS is in contact state 1, then there is,

$$\begin{cases} F_p^{L1} + F_a^{L1} = \sum_{i=1}^{M_{bL}} Q_{si}^{L1} \sin\theta_{si}^{L1} \cos\alpha \\ F_p^{R1} - F_a^{R1} = \sum_{i=1}^{M_{bR}} Q_{si}^{R1} \sin\theta_{si}^{R1} \cos\alpha \\ F_a^{L1} + F_a^{R1} = F_a \\ \left(F_p^{L1} + F_a^{L1}\right)^{\frac{2}{3}} + \left(F_p^{R1} - F_a^{R1}\right)^{\frac{2}{3}} = 2\left(F_p^{L1}\right)^{\frac{2}{3}} \end{cases} \tag{2}$$

If in contact state 2, there is,

$$\begin{cases} F_p^{L2} + F_a^{L2} = \sum_{i=1}^{M_{bL}} Q_{si}^{L2} \sin\theta_{si}^{L2} \cos\alpha \\ F_a^{R2} - F_p^{R2} = \sum_{i=1}^{M_{bR}} Q_{si}^{R2} \sin\theta_{si}^{R2} \cos\alpha \\ F_a^{L2} + F_a^{R2} = F_a \\ \left(F_p^{L2} + F_a^{L2}\right)^{\frac{2}{3}} - \left(F_p^{L2}\right)^{\frac{2}{3}} = \left(F_p^{R2}\right)^{\frac{2}{3}} + \left(F_a^{R2} - F_p^{R2}\right)^{\frac{2}{3}} \end{cases} \tag{3}$$

Considering the actual contact area, the wear depth between the ball and the screw/nut raceway h'_{sbs}/h'_{sbn} can be expressed as follows, respectively.

$$h'_{sbs}(t) = \frac{C_{b-s}(t) V_{b-s}(t)}{A_s} A_{rs} \tag{4}$$

$$h'_{sbn}(t) = \frac{C_{b-n}(t) V_{b-n}(t)}{A_n} A_{rn} \tag{5}$$

where $C_{b-s}(t)/C_{b-n}(t)$ is the number of cycles, A_k is the elliptical contact area, and A_{rk} is the actual contact area [16], expressed as follows:

$$A_k = \pi\, a_k\, b_k = \pi\left(\frac{6N_H R_k Q_k}{\pi E^*}\right)^{2/3} \tag{6}$$

$$A_{rk} = \left[\frac{\left(\frac{4}{\pi E^*}\frac{r_k r}{r_k - r}\right)}{\pi\left(r_k - r\right)}\right]^{\left(\frac{1}{r} - \frac{1}{r_k}\right)} \frac{D_f}{2 - D_f} a_{Lk} \tag{7}$$

D_f is the fractal parameter, $D_f = 1.62$.

Combining Eqs. (4)–(7), the wear depth between the ball and raceway h_{sbs}/h_{sbn} can be obtained.

$$h_{sbs}(t) = \frac{2C_{b-s}(t) V_{b-s}(t) b_s}{A_s L_{b-s}} A_{rs} \tag{8}$$

$$h_{sbn}(t) = \frac{2C_{b-n}(t) V_{b-n}(t) b_n}{A_n L_{b-n}} A_{rn} \tag{9}$$

where $L_{b-s} = L_s/\sin\alpha$, $L_{b-n} = L_{nL}/\sin\alpha = L_{nR}/\sin\alpha$.

The accumulated wear depth of BS in the travel direction is its accuracy decay value [10, 16, 36]. Then, the accuracy degradation model between the ball and the raceway under non-constant conditions is expressed as follows.

$$H_{sbs} = \frac{\cos\alpha}{\sin\theta_{si}^{uc}} \int_0^{L_{b-s}} \frac{C_{b-s}(t) V_{b-s}(t)}{L_{b-s}} \left(\frac{b_s^{Lc}}{A_s^{Lc}} A_{rs}^{Lc} + \frac{b_s^{Rc}}{A_s^{Rc}} A_{rs}^{Rc}\right) dl \tag{10}$$

$$H_{sbn} = \frac{\cos\alpha}{\sin\theta_{ni}^{uc}} \int_0^{L_{b-n}} \frac{C_{b-n}(t) V_{b-n}(t)}{L_{b-n}} \left(\frac{b_n^{Lc}}{A_n^{Lc}} A_{rn}^{Lc} + \frac{b_n^{Rc}}{A_n^{Rc}} A_{rn}^{Rc}\right) dl \tag{11}$$

However, in Eqs. (8) and (9), there are unknown quantities $V_{b-s}(t)/V_{b-n}(t)$, which need to be derived and solved by the following equations.

When the ball moves from the position of the No. i ball to the position of the No. $i+1$ ball, that is, from time t_{ssi} to time t_{ssi+1}, the wear amount between the ball and the screw raceway is obtained.

$$\begin{aligned} V_{b-si}\left(t_{ssi}\right) &= \int_{t_{ssi}}^{t_{ssi+1}} v_{b-si}\left(t_{ssi}\right) dt \\ &= \int_{t_{ssi}}^{t_{ssi+1}} K_{b-s} \frac{Q_{si}\left(t_{ssi}\right)}{H_{b-s}} \frac{R_{bsi}\left(t_{ssi}\right)\omega_{si-b}\left(t_{ssi}\right) r\cos\alpha}{\pi\left[1 + R_{bsi}\left(t_{ssi}\right)\right] v_{bs-ssi}\left(t_{ssi}\right) R} \\ &\quad \sqrt{R^2 + \left(\frac{L}{2\pi}\right)^2} \sqrt{\left(R - r\cos\theta_{si}\right)^2 + \left(\frac{L}{2\pi}\right)^2} dt \end{aligned} \tag{12}$$

According to Eq. (12), the wear amount between the first ball and the screw raceway in the whole cycle can be obtained. And it is recorded as $V_{b-s}^1(t)$, namely,

$$\begin{aligned} V_{b-s}^1(t) = {} & V_{b-s1}\left(t_{ss1}\right) + V_{b-s2}\left(t_{ss2}\right) + \ldots \\ & + V_{b-si}\left(t_{ssi}\right) + \ldots + V_{b-sM}\left(t_{ssM}\right) \end{aligned} \tag{13}$$

Then, the wear between all the balls and the screw can be summed by the Eq. (14). And it is recorded as $V_{b-s}(t)$, namely,

$$V_{b-s}(t) = V_{b-s}^1(t) + V_{b-s}^2(t) + \ldots + V_{b-s}^i(t) + \ldots + V_{b-s}^M(t) \tag{14}$$

In the same way, the wear amount $V_{b-n}^{1}(t)$ between the first ball and the nut raceway can be obtained in the whole cycle period.

$$V_{b-n}^{1}(t) = V_{b-n1}\left(t_{ns1}\right) + V_{b-n2}\left(t_{ns2}\right) + \cdots + V_{b-ni}\left(t_{nsi}\right) + \ldots + V_{b-nM}\left(t_{nsM}\right) \tag{15}$$

Then, the wear $V_{b-n}(t)$ between all the balls and the nut can be summed by the Eq. (16).

$$V_{b-n}(t) = V_{b-n}^{1}(t) + V_{b-n}^{2}(t) + \ldots + V_{b-n}^{i}(t) + \ldots + V_{b-n}^{M}(t) \tag{16}$$

According to Eqs. (14) and (16), the accuracy degradation model of the BS under non-constant operating conditions can be established.

$$\begin{cases} V(t)=V_{b-s}(t) + V_{b-n}(t) = \left[V_{b-s}^{L}(t) + V_{b-s}^{R}(t)\right] + \left[V_{b-n}^{L}(t) + V_{b-n}^{R}(t)\right] \\ H_s = H_{sbs} + H_{sbn} \end{cases} \tag{17}$$

Based on Eq. (18), considering single non-constant axial load condition, the accuracy decay model of the BS can be obtained under AL.

$$\begin{cases} V^{f}(t)=V_{b-s}^{f}(t) + V_{b-n}^{f}(t) = \left[V_{b-s}^{fL}(t) + V_{b-s}^{fR}(t)\right] + \left[V_{b-n}^{fL}(t) + V_{b-n}^{fR}(t)\right] \\ H_s^{f} = H_{sbs}^{f} + H_{sbn}^{f} \end{cases} \tag{18}$$

Among them, $V_{b-s}^{fL}(t)/V_{b-s}^{fR}(t)$ is the wear amount between the balls in the left/right nut and the screw under a single non-constant load condition. And they can be deduced refer to the derivation process of Eq. (14). $V_{b-n}^{fL}(t)/V_{b-n}^{fR}(t)$ is the wear amount between the balls and the left/right nut. And they can be also deduced refer to the derivation process of Eq. (16).

Similarly, the accuracy decay model of the BS can be also obtained considering single non-constant feed rate condition.

$$\begin{cases} V^{v}(t)=V_{b-s}^{v}(t) + V_{b-n}^{v}(t) = \left[V_{b-s}^{vL}(t) + V_{b-s}^{vR}(t)\right] + \left[V_{b-n}^{vL}(t) + V_{b-n}^{vR}(t)\right] \\ H_s^{v} = H_{sbs}^{v} + H_{sbn}^{v} \end{cases} \tag{19}$$

In Eq. (19), $V_{b-s}^{vL}(t)/V_{b-s}^{vR}(t)$ is the wear amount between the balls in the left/right nut and the screw under FR. $V_{b-n}^{vL}(t)/V_{b-n}^{vR}(t)$ is the wear amount between the balls and the left/right nut.

2.2 Accuracy decay modeling for rolling motion under non-constant conditions

Based on the analysis of rolling contact behavior [37, 38], it is shown that there are partial sliding and partial sticking phenomena in the contact area. Combined with the rolling contact analysis [39], the rolling wear between the ball and the screw/nut raceway can be modeled and analyzed.

$$\Delta h_{rbs}(t) = K_{b-s}\frac{F_{si}(t)}{A(\zeta)} v_{rbs}(t)\Delta t \tag{20}$$

where $A(\zeta)$ is the creep area parameter.

$$A(\zeta) \approx \frac{1}{8}\left[\frac{6N_H R_k Q_k(t)}{\pi E^*}\right]^{2/3} \tag{21}$$

According to Eq. (20), the rolling wear depth between the ball and the screw raceway can be obtained at time t_i.

$$h_{rbs} = h_{rbs}(t_{i-1}) + K_{b-s}\frac{F_{si}(t)}{A(\zeta)}\left\|S_{bs}(ti) - S_{bs}(t_{s-1})\right\| \tag{22}$$

Among them, $h_{rbs}\left(t_{i-1}\right)$ is the rolling wear depth between a ball and screw raceway at time t_{i-1}. According to Eqs. (21) and (22), at time t_i^{xs}, the cumulative rolling wear depth between the ball and the screw for the rolling contact area can be obtained.

$$h_{rbs}^{xs} = h_{rbs}^{xs}\left(t_A^{xs}\right) + \int_{t_A^{xs}}^{t_i^{xs}} K_{b-s}\frac{F_{si}}{A(\zeta_{xs})} v_{rbs}^{xs}\, dt_i^{xs},\ t_i^{xs} < {}^{xs}_{C} \tag{23}$$

Combined with Eq. (23), the rolling wear depth between the ball and the screw raceway in the x_s direction can be obtained; see Eq. (24).

$$h_{rbs}^{xs} = h_{rbs}^{xs}\left(t_A^{xs}\right) + \int_{l_A^{xs}}^{l_C^{xs}} K_{b-s}\frac{F_{si}}{A(\zeta_{xs})} v_{rbs}^{xs}\frac{dl_{xs}}{v_{b-s}^{xs}} \tag{24}$$

Among them, when contacting point A_{xs}, z $l_A^{xs} = 0$, when contacting point C_{xs}, $l_C^{xs} = 2a_{xs}$ [21].

The relationship between the rolling wear depth $h_{rbs}^{xs}(n)$ and the number of rolling contacts n can be expressed as follows.

$$h_{rbs}^{xs}(n) = h_{rbs}^{xs}(n-1) + \int_{l_A^{xs}(n)}^{l_C^{xs}(n)} K_{b-s}\frac{F_{si}}{A(\zeta_{xs})} v_{rbs}^{xs}(n)\frac{dl_{xs}}{v_{b-s}^{xs}} \tag{25}$$

Similarly, there is also creep phenomenon between the balls and the screw raceway in the y_s direction. The expressions for the rolling wear depth and the rolling number can also be obtained.

$$h_{rbs}^{ys}(n) = h_{rbs}^{ys}(n-1) + \int_{l_A^{ys}(n)}^{l_C^{ys}(n)} K_{b-s}\frac{F_{si}}{A(\zeta_{ys})} v_{rbs}^{ys}(n)\frac{dl_{ys}}{v_{b-s}^{ys}} \tag{26}$$

Because of the rolling wear depth between the balls in the left/right nut and the screw raceway, the accuracy decay value can be obtained in the x_s direction from Eqs. (27) and (28), respectively.

$$\begin{cases} h_{r-xs}^{Lc}(n) = \sum_{i=1}^{n_{xs}} \frac{K_{b-s} a_{xs} F_{si}^{Lc}(t)\, \zeta_{xs}^{Lc}(t)\, v_{b-si}^{xs}(t)}{4 c_{xs} a_{ys}} \\ H_{r-xs}^{Lc} = \frac{\cos\alpha}{\sin\theta_{si}^{Lc}} \int_0^{L_{b-s}} h_{r-xs}^{Lc}(n)\, dl \end{cases} \tag{27}$$

$$\begin{cases} h_{r-xs}^{Rc}(n) = \sum_{i=1}^{n_{xs}} \frac{K_{b-s} a_{xs} F_{si}^{Rc}(t)\, \zeta_{xs}^{Rc}(t)\, v_{b-si}^{xs}(t)}{4 c_{xs} a_{ys}} \\ H_{r-xs}^{Rc} = \frac{\cos\alpha}{\sin\theta_{si}^{Rc}} \int_0^{L_{b-s}} h_{r-xs}^{Rc}(n)\, dl \end{cases} \tag{28}$$

In Eqs. (27) and (28), c is determined by the axial load and the preload. According to Sect. 2.1, when the axial load is less than 2.83 times the preload, $c=1$, and when the axial load is greater than 2.83 times the preload, $c=2$.

Similarly, due to the rolling wear depth between the balls in the left/right nut and the screw raceway, the accuracy decay value can be obtained in the y_s direction from Eqs. (29) and (30), respectively.

$$\begin{cases} h_{r-ys}^{Lc}(n) = \sum_{i=1}^{n_{ys}} \frac{K_{b-s} F_{si}^{Lc}(t)\, a_{ys} \zeta_{ys}^{Lc}(t)\, (\delta_{si}^{Lc} - r) r\omega_t(t)}{4 c_{ys} a_{xs}} \\ H_{r-ys}^{Lc} = \frac{\cos\alpha}{\sin\theta_{si}^{Lc}} \int_0^{L_{b-s}} h_{r-ys}^{Lc}(n)\, dl \end{cases} \tag{29}$$

$$\begin{cases} h_{r-ys}^{Rc}(n) = \sum_{i=1}^{n_{ys}} \frac{K_{b-s} F_{si}^{Rc}(t)\, a_{ys} \zeta_{ys}^{Rc}(t)\, (\delta_{si}^{Rc} - r) r\omega_t(t)}{4 c_{ys} a_{xs}} \\ H_{r-ys}^{Rc} = \frac{\cos\alpha}{\sin\theta_{si}^{Rc}} \int_0^{L_{b-s}} h_{r-ys}^{Rc}(n)\, dl \end{cases} \tag{30}$$

Then, the rolling wear depth $h_{r-xn}^{Lc}(n)/h_{r-xn}^{Rc}(n)$ and the BS accuracy decay value $H_{r-xn}^{Lc}/H_{r-xn}^{Rc}$ in the x_n direction can be solved by the following equations, respectively.

$$\begin{cases} h_{r-xn}^{Lc}(n) = \sum_{i=1}^{n_{xn}} \frac{K_{b-n} a_{xn} F_{ni}^{Lc}(t)\, \zeta_{xn}^{Lc}(t)\, v_{b-n}^{xn}(t)}{4 c_{xn} a_{yn}} \\ H_{r-xn}^{Lc} = \frac{\cos\alpha}{\sin\theta_{ni}^{Lc}} \int_0^{L_{b-n}} h_{r-xn}^{Lc}(n)\, dl \end{cases} \tag{31}$$

$$\begin{cases} h_{r-xn}^{Rc}(n) = \sum_{i=1}^{n_{xn}} \frac{K_{b-n} a_{xn} F_{ni}^{Rc}(t)\, \zeta_{xn}^{Rc}(t)\, v_{b-n}^{xn}(t)}{4 c_{xn} a_{yn}} \\ H_{r-xn}^{Rc} = \frac{\cos\alpha}{\sin\theta_{ni}^{Rc}} \int_0^{L_{b-n}} h_{r-xn}^{Rc}(n)\, dl \end{cases} \tag{32}$$

The accuracy decay value caused by the rolling wear depth between the ball and the left/right nut in the y_n direction can be solved by Eqs. (33) and (34), respectively.

$$\begin{cases} h_{r-yn}^{Lc}(n) = \sum_{i=1}^{n_{yn}} \frac{K_{b-n} F_{ni}^{Lc}(t)\, a_{yn} \zeta_{yn}^{Lc}(t)\, (r - \delta_a^{Lc})\, r\omega_t(t)}{4 c_{yn} a_{xn}} \\ H_{r-yn}^{Lc} = \frac{\cos\alpha}{\sin\theta_{ni}^{Lc}} \int_0^{L_{b-n}} h_{r-yn}^{Lc}(n)\, dl \end{cases} \tag{33}$$

$$\begin{cases} h_{r-yn}^{Rc}(n) = \sum_{i=1}^{n_{yn}} \frac{K_{b-n} F_{ni}^{Rc}(t)\, a_{yn} \zeta_{yn}^{Rc}(t)\, (r - \delta_a^{Rc})\, r\omega_t(t)}{4 c_{yn} a_{xn}} \\ H_{r-yn}^{Rc} = \frac{\cos\alpha}{\sin\theta_{ni}^{Rc}} \int_0^{L_{b-n}} h_{r-yn}^{Rc}(n)\, dl \end{cases} \tag{34}$$

3 Accuracy decay analysis for mixed sliding-rolling motion under non-constant operation conditions

3.1 Accuracy decay analysis for mixed sliding-rolling motion under AL

The ball screw parameters studied are shown in Table 1.

Considering the mixed sliding-rolling motion, combined with Eqs. (18), (27)–(34), the accuracy decay model can be obtained under AL.

$$\begin{cases} V^f(t) = V_{b-s}^f(t) + V_{b-n}^f(t) = \left[V_{b-s}^{fL}(t) + V_{b-s}^{fR}(t)\right] + \left[V_{b-n}^{fL}(t) + V_{b-n}^{fR}(t)\right] \\ H_s^f = H_{sbs}^f + H_{sbn}^f \\ H_r^f = H_{r-xs}^{Lcf} + H_{r-xs}^{Rcf} + H_{r-ys}^{Lcf} + H_{r-ys}^{Rcf} + H_{r-xn}^{Lcf} + H_{r-xn}^{Rcf} + H_{r-yn}^{Lcf} + H_{r-yn}^{Rcf} \\ H^f = H_s^f + H_r^f \end{cases} \tag{35}$$

Table 1 Ball screw parameters

Parameters	Value	Unit
Nominal diameter of ball screw	50	mm
Ball diameter	6.75	mm
Nut track curvature radius	3.673	mm
Screw track curvature radius	3.673	mm
Contact angle	45	degree
Helix angle	4.35	degree
Lead	12	mm
Axial length of nuts	80	mm
Number of balls	136	/
Rows × Turns × Leads	2 × 2.5 × 1	/
Raceway curvature ratio	1.09	/
Screw hardness	62	HRC
Nut hardness	62	HRC
Young's modulus	205	GPa
Poisson's ratio	0.3	/
Lubrication mode	Grease	/
Boundary wear coefficient	3.2E-11	/

Three sets of different AL are set separately, $[0.5 * \sin(\pi t/180) + 0.5]$ kN, $[1 * \sin(\pi t/180) + 1]$ kN, and $[1.5 * \sin(\pi t/180) + 1.5]$ kN. And the decay characteristics of the preload are also considered [40]. The accuracy degradation of the BS for mixed sliding-rolling motion is analyzed under three different AL, respectively, in order to reveal its accuracy decay mechanism. Figure 2a, b shows the accuracy decay behavior between the balls in the left/right nut and the screw raceway for mixed sliding-rolling motion under three different. It is the combined effect of the accuracy decay value caused by $V_{b-s}^{fL}(t)$, $V_{b-s}^{fR}(t)$ and the sum of H_{r-xs}^{Lcf}, H_{r-xs}^{Rcf}, H_{r-ys}^{Lcf},H_{r-ys}^{Rcf}. Figure 2c, d shows the

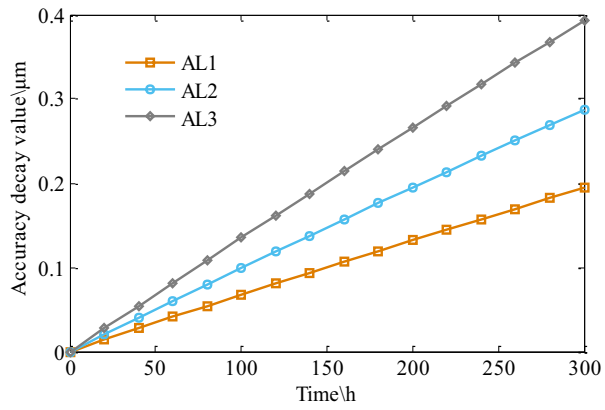

(a) Between the ball in the left nut and the screw

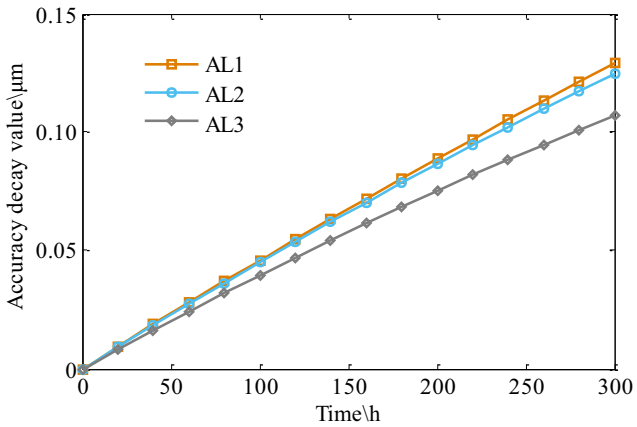

(b) Between the ball in the right nut and the screw

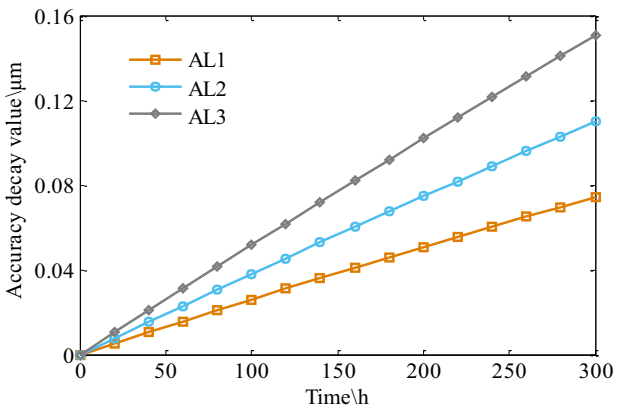

(c) Between the ball and the left nut

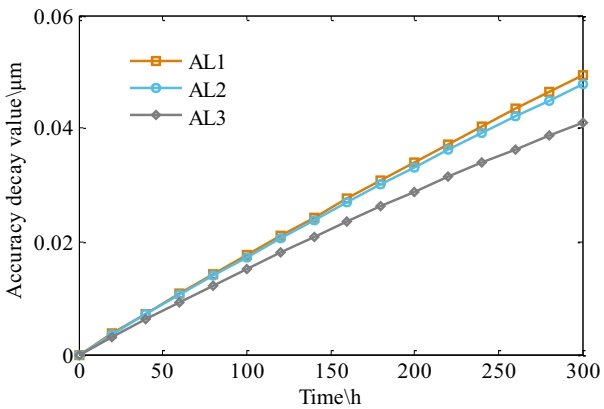

(d) Between the ball and the right nut

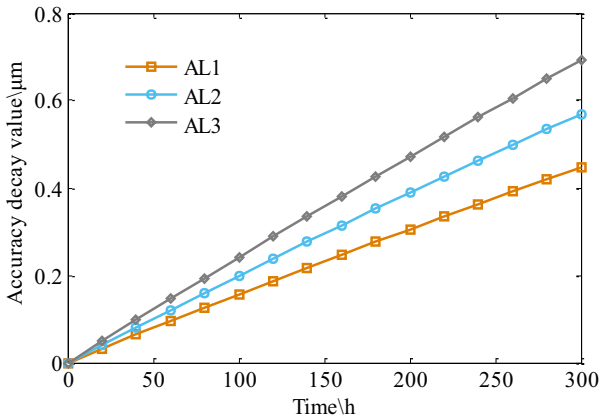

(e) Accuracy degradation value

Fig. 2 Accuracy degradation for mixed sliding-rolling motion under AL. **a** Between the ball in the left nut and the screw. **b** Between the ball in the right nut and the screw. **c** Between the ball and the left nut. **d** Between the ball and the right nut. **e** Accuracy degradation value

accuracy decay characteristics between the balls and the left/right nut for mixed sliding-rolling motion. It is the combined effect of the accuracy decay value caused by $V_{b-n}^{fL}(t)$, $V_{b-n}^{fR}(t)$ and the sum of H_{r-xn}^{Lcf}, H_{r-xn}^{Rcf}, H_{r-yn}^{Lcf},H_{r-yn}^{Rcf}. Figure 2e shows the total accuracy decay value of the BS, which is H^f in Eq. (28).

According to Fig. 2a, c, when the amplitude of non-constant axial load increases, the accuracy decay value between the ball in the left nut and the screw/nut raceway increases considering the mixed sliding-rolling motion. However, according to Fig. 2b, d, the accuracy decay value between the ball in the right nut and the screw/nut raceway decreases considering the mixed sliding-rolling motion, when the non-constant load amplitude is expanded. According to Fig. 2e, the analysis results are as follows. When the BS is in different amplitudes of AL in the same simulated test period, the accuracy degradation due to rolling motion between the ball and raceway accounted for 19.81%, 20.33%, and 20.76% of the BS accuracy loss due to sliding motion, respectively. And the accuracy degradation due to rolling motion between the ball and raceway accounted for 16.53%, 16.90%, and 17.19% of the BS total accuracy loss due to mixed sliding-rolling motion, respectively. It can be observed that when the amplitude of the AL increases, the proportion of the accuracy loss value due to rolling wear depth increases gradually.

3.2 Accuracy decay analysis for mixed sliding-rolling motion under FR

Considering the mixed sliding-rolling motion, combined with Eqs. (19), (27)–(34), the accuracy decay model can be obtained under FR.

$$\begin{cases} V^v(t) = V_{b-s}^v(t) + V_{b-n}^v(t) = \left[V_{b-s}^{vL}(t) + V_{b-s}^{vR}(t)\right] + \left[V_{b-n}^{vL}(t) + V_{b-n}^{vR}(t)\right] \\ H_s^v = H_{sbs}^v + H_{sbn}^v \\ H_r^v = H_{r-xs}^{Lcv} + H_{r-xs}^{Rcv} + H_{r-ys}^{Lcv} + H_{r-ys}^{Rcv} + H_{r-xn}^{Lcv} + H_{r-xn}^{Rcv} + H_{r-yn}^{Lcv} + H_{r-yn}^{Rcv} \\ H^v = H_s^v + H_r^v \end{cases} \tag{36}$$

Three sets of different FR are set separately, $[0.5 * \sin(\pi t/180) + 0.5]$ rad/s, $[1 * \sin(\pi t/180) + 1]$ rad/s, $[1.5 * \sin(\pi t/180) + 1.5]$ rad/s. The accuracy degradation of the BS for mixed sliding-rolling motion under three different FR are analyzed, respectively. Figure 3b shows the accuracy decay between the balls in the left/right nut and the screw raceway for mixed sliding-rolling motion under three sets of different FR. It is the combined effect of the accuracy decay value caused by $V_{b-s}^{vL}(t)$, $V_{b-s}^{vR}(t)$ and the sum of H_{r-xs}^{Lcv}, H_{r-xs}^{Rcv}, H_{r-ys}^{Lcv},H_{r-ys}^{Rcv}. Figure 3c, d shows the accuracy decay characteristics between the balls and the left/right nut for mixed sliding-rolling motion. It is the combined effect of the accuracy decay value caused by $V_{b-n}^{vL}(t)$, $V_{b-n}^{vR}(t)$ and the sum of H_{r-xn}^{Lcv}, H_{r-xn}^{Rcv}, H_{r-yn}^{Lcv},H_{r-yn}^{Rcv}. Figure 3e shows the total accuracy decay value of the BS, which is H^v in Eq. (36).

From Fig. 3a–e, the following conclusions can be drawn. By comparing the accuracy decay considering pure sliding motion, the accuracy degradation of the BS for mixed sliding-rolling motion under FR also have a similar trend in Fig. 3a, b. That is, with the increase of the feed rate amplitude, the accuracy decay value of the BS also increases. But the difference is that the total accuracy decay value of the BS increases slightly when the mixed sliding-rolling motion is considered. According to Fig. 3c–e, the analysis results are as follows. When the ball screw is in different amplitudes of FR in the same simulated test period, the accuracy decay value due to rolling motion between the ball and raceway accounted for 19.92%, 20.47%, and 20.93% of the BS accuracy loss due to sliding motion, respectively. And the accuracy decay value due to rolling motion between the ball and raceway accounted for 16.61%, 16.99%, and 17.31% of the BS accuracy loss due to mixed sliding-rolling motion. It can be observed that when the amplitude of the FR increases, the proportion of the accuracy loss value due to rolling wear increases gradually. Because the creep rate between the balls and the screw/nut raceways increases slightly as the amplitude of the FR increases.

3.3 Accuracy decay analysis for mixed sliding-rolling motion under AL + FR

Considering the mixed sliding-rolling motion, combined with Eqs. (17), (27)–(34), the accuracy decay model can be obtained under AL + FR.

$$\begin{cases} V(t) = V_{b-s}(t) + V_{b-n}(t) = \left[V_{b-s}^{L}(t) + V_{b-s}^{R}(t)\right] + \left[V_{b-n}^{L}(t) + V_{b-n}^{R}(t)\right] \\ H_s = H_{sbs} + H_{sbn} \\ H_r = H_{r-xs}^{Lc} + H_{r-xs}^{Rc} + H_{r-ys}^{Lc} + H_{r-ys}^{Rc} + H_{r-xn}^{Lc} + H_{r-xn}^{Rc} + H_{r-yn}^{Lc} + H_{r-yn}^{Rc} \\ H^{fv} = H_s + H_r \end{cases} \tag{37}$$

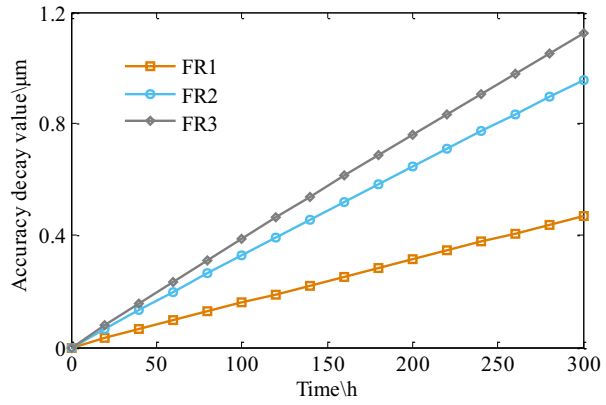

(a) Between the ball in the left nut and the screw

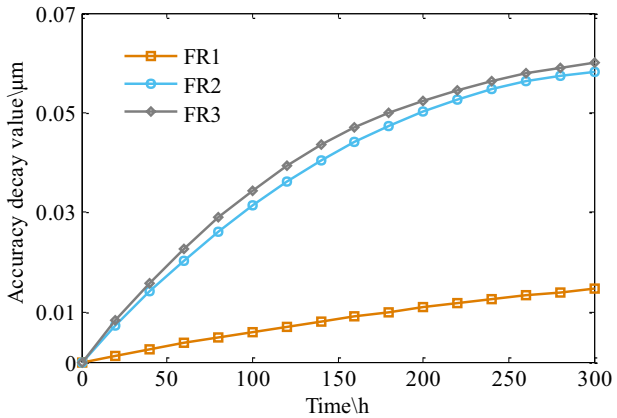

(b) Between the ball in the right nut and the screw

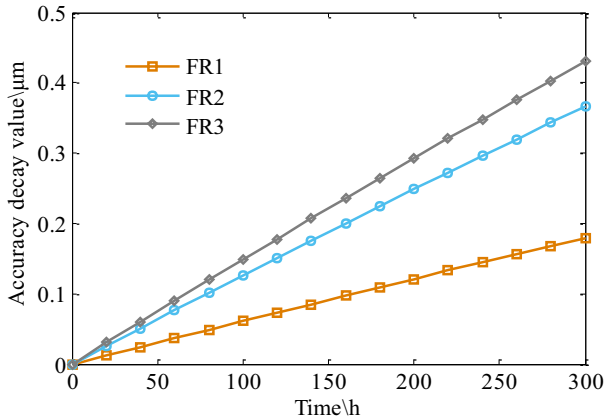

(c) Between the ball and the left nut

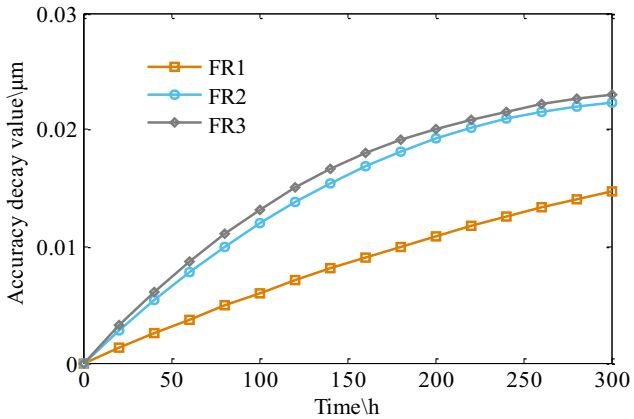

(d) Between the ball and the right nut

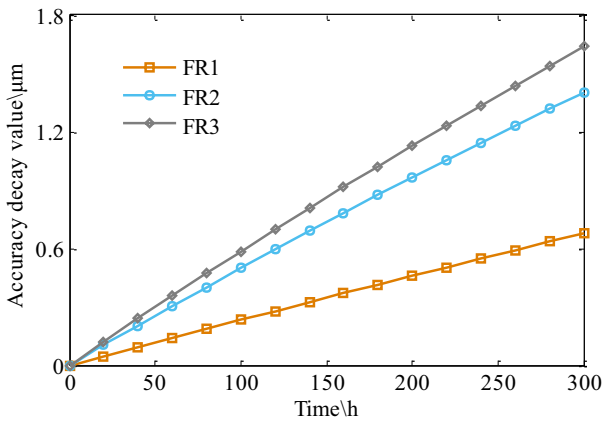

(e) Accuracy degradation value

Fig. 3 Accuracy degradation considering mixed sliding-rolling motion under FR. **a** Between the ball in the left nut and the screw. **b** Between the ball in the right nut and the screw. **c** Between the ball and the left nut. **d** Between the ball and the right nut. **e** Accuracy degradation value

Three groups of complex non-constant operation conditions are set, the combination of $[0.5 * \sin(\pi t/180) + 0.5]$ kN and $[0.5 * \sin(\pi t/180) + 0.5]$ rad/s is used as the first group, the second group is the combination of $[1 * \sin(\pi t/180) + 1]$ kN and $[1 * \sin(\pi t/180) + 1]$ rad/s, nd the third group is the combination of $[1.5 * \sin(\pi t/180) + 1.5]$ kN and $[1.5 * \sin(\pi t/180) + 1.5]$ rad/s. Figure 4a, b shows the accuracy decay between the balls in the left/right nut and the screw raceway for mixed sliding-rolling motion under three

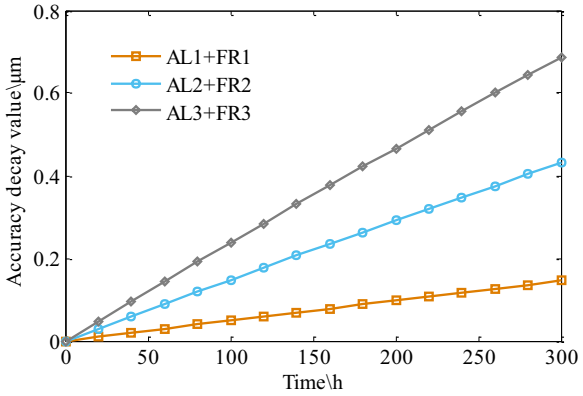

(a) Between the ball in the left nut and the screw

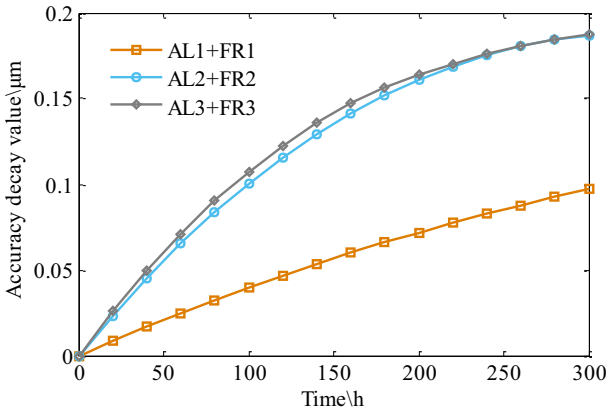

(b) Between the ball in the right nut and the screw

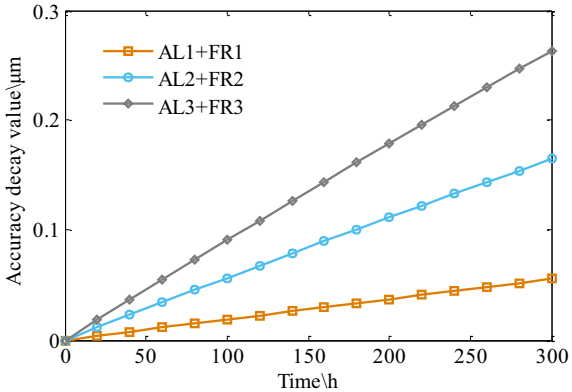

(c) Between the ball and the left nut

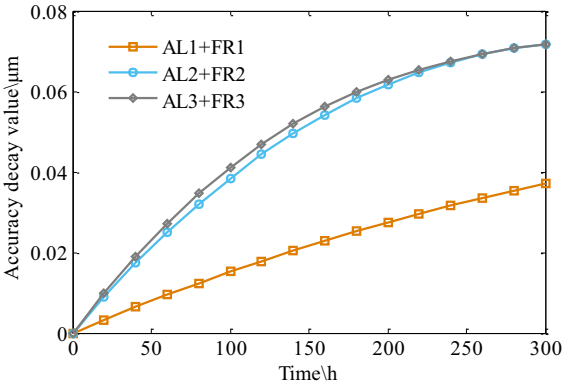

(d) Between the ball and the right nut

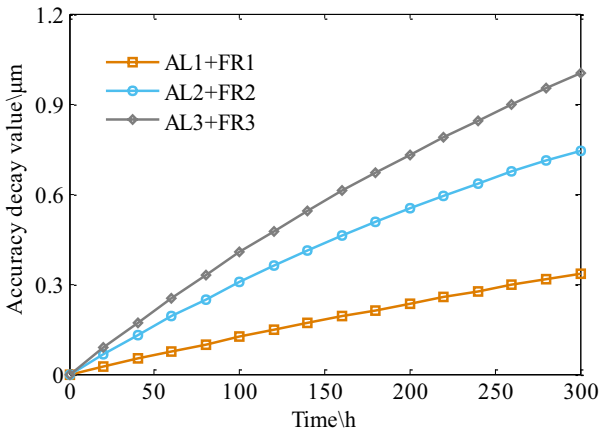

(e) Accuracy degradation value

Fig. 4 Accuracy degradation for mixed sliding-rolling motion under AL+FR. **a** Between the ball in the left nut and the screw. **b** Between the ball in the right nut and the screw. **c** Between the ball and the left nut. **d** Between the ball and the right nut. **e** Accuracy degradation value

groups of AL+FR. It is the combined effect of the accuracy decay value caused by $V_{b-s}^{L}(t)$, $V_{b-s}^{R}(t)$ and the sum of H_{r-xs}^{Lc}, H_{r-xs}^{Rc}, H_{r-ys}^{Lc}, H_{r-ys}^{Rc}. Figure 4c, d shows the accuracy decay between the balls and the left/right nut. It is the combined effect of the accuracy decay value caused by $V_{b-n}^{L}(t)$, $V_{b-n}^{R}(t)$ and the sum of H_{r-xn}^{Lc}, H_{r-xn}^{Rc}, H_{r-yn}^{Lc}, H_{r-yn}^{Rc}. Figure 4e shows the total accuracy decay value of the BS, which is H^{fv} in Eq. (30).

From Fig. 4a–e, the following conclusions can be drawn: when the accuracy degradation considering pure sliding motion is compared, the accuracy degradation characteristics of the BS for mixed sliding-rolling motion under AL + FR also have consistent trend of change. That is, with the amplitude increase of the axial load and feed rate, it does not matter whether the BS is during pure sliding or mixed sliding-rolling motion, its accuracy decay value increase. According to Fig. 4c–e, it can be observed that the proportion of rolling wear fluctuates when the BS is during different groups of AL + FR. The accuracy decay value due to rolling motion between the ball and raceway accounted for 18.16%, 18.58%, and 19.21% of the BS accuracy loss due to sliding motion, respectively. And the accuracy degradation due to rolling motion between the ball and raceway accounted for 15.37%, 15.67%, and 16.11% of the BS accuracy loss due to mixed sliding-rolling motion, respectively. The proportion of rolling wear gradually increased slightly. On the one hand, it is because when the amplitude of AL increases, the contact load between the ball and the nut raceway decreases. On the other hand, the reason is that the creep rate between the ball and the screw raceway increases. Additionally, the creep rates between the balls and the screw/nut raceways increase as the amplitude of FR increases. As a result, the proportion of rolling wear depth between the balls and the screw/nut raceways to the total accuracy decay value increases.

4 Accuracy decay experiment test for mixed sliding-rolling motion under non-constant operation conditions

4.1 Accuracy decay experimental research for mixed sliding-rolling motion under AL

The accuracy decay test principle is adapted from references [16] and [21]. While the accuracy decay test procedure is adapted from reference [26]. In the accuracy degradation test, V_μ (the test feed stroke of the ball screw, i–e, 400 mm) is used as the accuracy degradation index of the BS. Before the experiment, the initial value V_μ^0 is tested, recorded, and used as the initial value of the positioning accuracy. Then, V_μ^t is tested and recorded at different time points according to the test procedure. The difference between V_μ^t and V_μ^0 is calculated, the accuracy degradation value of the BS can be obtained.

The experimental steps include the following: (1) The ball screw rotating is observed carefully. It is noticed that with an increase in the operation time, the accuracy slightly increases than the initial accuracy characteristics. According to Zhou et al. [10] and Liu et al. [16], the accuracy time of the ball screw during a running-in period is optimum at 157 h and 125 h. The result of Zhou differs from Liu's because of the time interval. Zhou set this interval at 157 h. After running for 157 h, the accuracy changed from the initial value of 7.82 to 6.14 μm. To reduce the error of the running-in period, 20 h is used in the presented study. After every 20 h, the ball screw accuracy test is performed to compare the initial value of the accuracy. The test is completed when the running-in period was 120 h. (2) After running in, the initial positioning error of the ball screw is noticed about 5 times, as shown in Table 2. The average value is obtained, and V_μ is used to estimate the accuracy decay index. (3) The parameters of the test conditions are set according to Sect. 3.1. These include the initial preload $F_p = 1330$ N and the feed rate $v = 240$ mm/min. In the experiment, the grease lubrication method (KOC301) is used at room temperature (23 ± 2 ℃). (4) The ball screw accuracy degradation test is carried out according to the non-constant load condition 1. After every 20 h, the laser interferometer is used to collect and record the positioning error of the BS. The lubricant is applied evenly throughout the test. (5) For the AL 2, the steps (1) to (4) are repeated with a new ball screw. For the AL 3, steps (1) to (4) are repeated, and the positioning accuracy test value is obtained. (6) The original positioning error of the BS and the positioning error after the test are calculated and analyzed under the single non-constant axial load condition.

Table 2 Initial positioning error

Number of tests	1	2	3	4	5
Positioning error/μm	8.633	8.634	8.635	8.634	8.634

In step (2), the initial positioning error of the BS was tested multiple times, which is shown in Table 2.

In step (5) and step (6), the accuracy test results of the BS under three different amplitudes of AL are tested. According to accuracy decay analysis for mixed sliding-rolling motion under AL, Fig. 5 shows the comparative results of the accuracy decay analysis and experimental test.

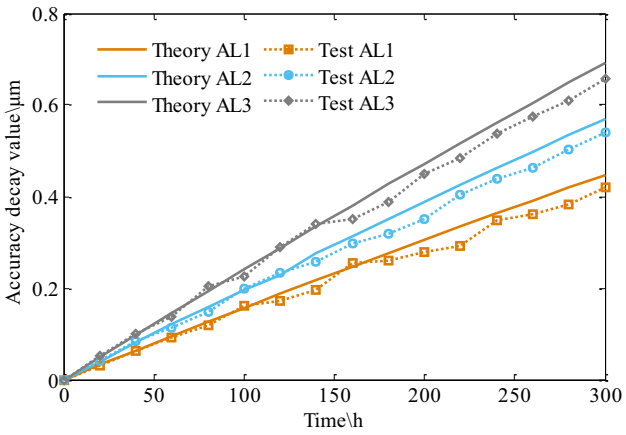

Fig. 5 Experimental analysis of accuracy decay for mixed sliding-rolling motion under AL

Table 3 Accuracy decay analysis for mixed sliding-rolling motion under AL

Time/h	Absolute error /μm			Relative error /%		
	AL 1	AL 2	AL 3	AL 1	AL 2	AL 3
20	−0.001	0.001	0.003	−3.03	2.50	6.12
40	0.001	0.003	0.001	1.59	3.70	1.02
60	−0.003	−0.008	−0.008	−3.16	−6.61	−5.48
80	−0.006	−0.012	0.010	−4.76	−7.50	5.15
100	0.004	0.003	−0.016	2.55	1.53	−6.64
120	−0.014	0.004	0.002	−7.49	1.75	0.69
140	−0.021	−0.019	0.005	−9.68	−6.86	1.50
160	0.007	−0.017	−0.028	2.83	−5.41	−7.37
180	−0.018	−0.034	−0.038	−6.50	−9.66	−8.90
200	−0.038	−0.037	−0.023	−12.42	−9.51	−4.87
220	−0.042	−0.033	−0.043	−12.54	−7.75	−8.32
240	−0.025	−0.034	−0.043	−6.89	−7.36	−7.66
260	−0.029	−0.046	−0.041	−7.42	−9.24	−6.78
280	−0.036	−0.042	−0.066	−8.59	−7.87	−10.17
300	−0.043	−0.050	−0.054	−9.62	−8.79	−7.80

The results of theoretical analysis and experimental test are shown in Table 3.

The following conclusions can be drawn from the analysis of Table 3. Considering mixed sliding-rolling motion under three different AL, the maximum value of the absolute error between theoretical model analysis and experimental test results was 0.043 μm, 0.050 μm, and 0.066 μm, and the minimum value of the absolute value of the absolute error is 0.001 μm, 0.001 μm, and 0.001 μm, respectively. And the average values of the absolute errors are about 0.0192 μm, 0.0229 μm, and 0.0254 μm, respectively. In addition, the maximum value of the relative error between theoretical model analysis and experimental test results was 12.54%, 9.66%, and 10.17%; the minimum value of the relative value of the relative error is 1.59%, 1.53%, and 1.02%, respectively. And the average values of the relative errors are about 6.60%, 6.40%, and 5.90%, respectively. Furthermore, when compared with the accuracy decay value under pure sliding motion, the conclusions are as follows. If the mixed sliding-rolling motion and different AL are considered comprehensively, the average values of the absolute errors were changed from 0.031 μm, 0.033 μm, and 0.038 μm to 0.0192 μm, 0.0229 μm, and 0.0254 μm, respectively. And the average values of the relative errors were changed from 12.66%, 11.40%, 11.38% to 6.60%, 6.40%, 5.90%. Then, both the average value of the absolute error and the average value of the relative error decrease. The summary shows that the accuracy decay analysis model established in this paper is beneficial to improve the prediction precision of BS accuracy decay.

4.2 Accuracy decay experimental research for mixed sliding-rolling motion under FR

According to accuracy decay analysis for mixed sliding-rolling motion under FR in Sect. 3.2, Fig. 6 shows the comparative results of the accuracy decay analysis and experimental test.

The results of theoretical analysis and experimental test are shown in Table 4.

From the analysis of Table 4, it can be seen that the following is entered. Considering mixed sliding-rolling motion under three different FR, the maximum value of the absolute error between theoretical model analysis and experimental test results was 0.068 μm, 0.163 μm, and 0.181 μm, and the

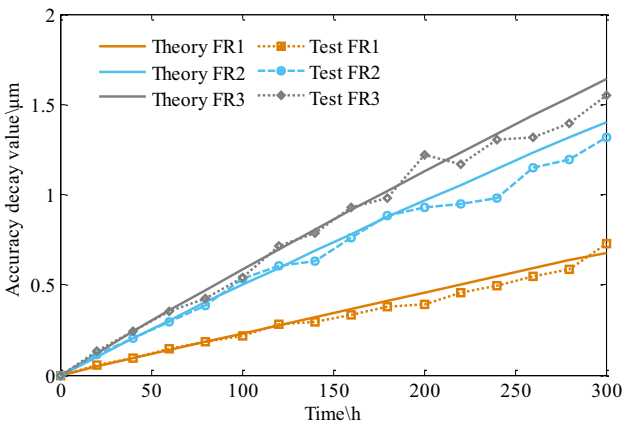

Fig. 6 Experimental analysis of accuracy decay for mixed sliding-rolling motion under FR

Table 4 Accuracy decay analysis for mixed sliding-rolling motion under FR

Time/h	Absolute error /μm			Relative error /%		
	FR 1	FR 2	FR 3	FR 1	FR 2	FR 3
20	0.005	0.009	0.014	10.64	8.74	11.57
40	0.002	0.001	0.005	2.15	0.49	2.08
60	0.004	−0.009	−0.006	2.86	−2.97	−1.68
80	−0.003	−0.019	−0.046	−1.61	−4.73	−9.75
100	−0.016	0.032	−0.047	−6.90	6.41	−8.03
120	0.004	0.011	0.020	1.44	1.85	2.87
140	−0.026	−0.059	−0.022	−8.05	−8.56	−2.73
160	−0.035	−0.022	0.011	−9.51	−2.81	1.20
180	−-0.034	0.008	−0.044	−8.23	0.91	−4.30
200	−0.068	−0.038	0.096	−14.85	−3.93	8.52
220	−0.047	−0.108	−0.063	−9.34	−10.24	−5.12
240	−0.055	−0.163	−0.161	−10.06	−14.07	−12.06
260	−0.047	−0.083	−0.141	−7.95	−6.74	−9.81
280	−0.052	−0.126	−0.181	−8.19	−9.56	−11.77
300	0.049	−0.136	−0.141	7.23	−9.69	−8.61

minimum value of the absolute value of the absolute error is 0.002 μm, 0.001 μm, and 0.005 μm, respectively. And the average values of the absolute errors are about 0.0298 μm, 0.0549 μm, and 0.0665 μm, respectively. Moreover, the maximum value of the relative error between theoretical model analysis and experimental test results was 10.64%, 14.07%, and 12.06%, and the minimum value of the relative value of the absolute error is 1.44%, 0.49%, and 1.20%. And the average values of the relative errors are about 7.27%, 6.11%, and 6.67%, respectively. Furthermore, when compared with the accuracy decay value under pure sliding motion, the conclusions are as follows. If the mixed sliding-rolling motion and different FR are considered comprehensively, the average values of the absolute errors were changed from 0.0238 μm, 0.0505 μm, and 0.0589 μm to 0.0298 μm, 0.0549 μm, and 0.0665 μm respectively. And the maximum values of the relative errors were changed from 33.34%, 31.77%, and 33.66% to 10.64%, 14.07%, and 12.06%; the average values of the relative errors were changed from 11.18%, 11.19%, 11.22% to 7.27%, 6.11%, and 6.67%, respectively. The analysis shows that the average of absolute error increased slightly, but the average value of relative error decreased. And the maximum value and the average value of the relative error decreased significantly. It shows that the accuracy decay analysis model proposed is beneficial to improve the BS prediction precision under different FR.

4.3 Accuracy decay experimental research for mixed sliding-rolling motion under AL + FR

According to accuracy decay analysis under AL + FR in Sect. 3.3, Fig. 7 shows the comparative results of the accuracy decay analysis and experimental test.

The results of theoretical analysis and experimental test are shown in Table 5.

It can be seen from the analysis of Table 5. When the BS is under three different combinations of time-varying axial load and feed rate, the maximum value of the absolute error between theoretical model analysis and experimental test results was 0.038 μm, 0.099 μm, and 0.136 μm, and the minimum value of the absolute value of the absolute error is 0.002 μm, 0.004 μm, and 0.004 μm. And the average values of the absolute errors are about 0.0169 μm, 0.0352 μm, and 0.0429 μm, respectively. Moreover, the maximum value of the relative error between theoretical model analysis and experimental test results was 16.17%, 14.26%, and 14.30%, and the minimum value of the relative value of the absolute error is 2.37%, 2.68%, and 0.99%, respectively. And the average values of the relative errors

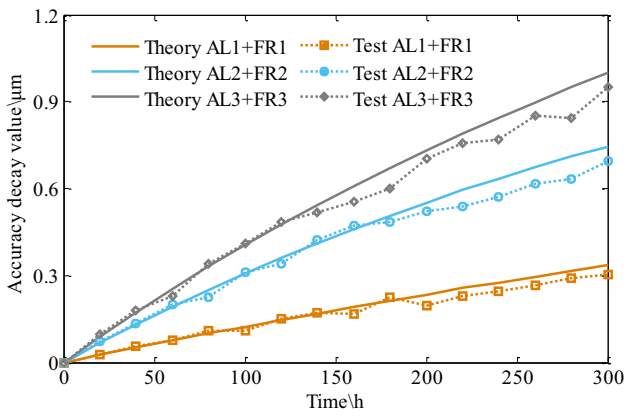

Fig. 7 Experimental analysis of accuracy decay for mixed sliding-rolling motion under AL + FR

Table 5 Accuracy decay analysis for mixed sliding-rolling motion under AL + FR

Time/h	Absolute error /μm			Relative error /%		
	AL + FR 1	AL + FR 2	AL + FR 3	AL + FR 1	AL + FR 2	AL + FR 3
20	0.002	0.006	0.009	7.69	9.09	10.23
40	0.004	0.004	0.006	7.84	3.08	3.47
60	0.003	0.008	−0.025	4.00	4.19	−9.88
80	0.009	−0.024	0.008	9.09	−9.60	2.42
100	−0.014	0.006	0.004	−11.38	1.96	0.99
120	0.006	−0.020	0.009	4.11	−5.56	1.89
140	0.004	0.011	−0.027	2.37	2.68	−4.97
160	−0.022	0.013	−0.056	−11.52	2.82	−9.20
180	0.011	−0.023	−0.073	5.16	−4.54	−10.88
200	−0.038	−0.031	−0.027	−16.17	−5.62	−3.70
220	−0.028	−0.055	−0.032	−10.94	−9.26	−4.06
240	−0.030	−0.063	−0.073	−10.87	−9.92	08.65
260	−0.028	−0.096	−0.075	−9.46	−14.26	−8.35
280	−0.025	−0.099	−0.136	−7.91	−13.94	−14.30
300	−0.030	−0.069	−0.083	−8.96	−9.26	−8.28

are about 8.50%, 7.05%, and 6.75%, respectively. In addition, when compared with the accuracy decay characteristics under pure sliding motion, the conclusions are as follows. If the mixed sliding-rolling motion and different AL + FR are considered comprehensively, the average values of the absolute errors were changed from 0.0074 μm, 0.0229 μm, and 0.0334 μm to 0.0169 μm, 0.0352 μm, and 0.0429 μm. And the maximum values of the relative errors were changed from 35.29%, 33.34%, and 38.36% to 16.17%, 14.26%, and 14.30%, and the average values of the relative errors were changed from 11.18%, 11.19%, and 11.22% to 8.50%, 7.05%, and 6.75%, respectively. Similarly, the average of absolute error increased slightly, but the average value of relative error decreased. Furthermore, the maximum value and the average value of the relative error decreased significantly. Therefore, the accuracy decay analysis model established is beneficial to improve the BS prediction precision under different AL + FR.

5 Conclusion

In this paper, considering mixed sliding-rolling motion in CNC machine tools, the numerical modeling method for the accuracy decay of the BS under single or multiple non-constant operating conditions is proposed. The model is verified and analyzed through experimental testing. The main conclusions of the research can be summarized as follows:

1. Under different AL, the accuracy degradation due to rolling motion between the ball and raceway accounted for 19.81%, 20.33%, and 20.76% of the ball screw accuracy loss due to sliding motion, respectively. And the accuracy degradation due to rolling motion between the ball and raceway accounted for 16.53%, 16.90%, and 17.19% of the ball screw accuracy loss due to mixed sliding-rolling motion, respectively. If the mixed sliding-rolling motion and different AL are considered comprehensively, the average values of the absolute errors were changed from 0.031 μm, 0.033 μm, and 0.038 μm to 0.0192 μm, 0.0229 μm, and 0.0254 μm, respectively. And the average values of the relative errors were changed from 12.66%, 11.40%, and 11.38% to 6.60%, 6.40%, and 5.90%, respectively.

2. Considering mixed slip-roll motion under FR, the accuracy degradation due to rolling motion between the ball and raceway accounted for 19.92%, 20.47%, and 20.93% of the BS accuracy loss due to sliding motion. And the accuracy degradation due to rolling motion between the ball and raceway accounted for 16.61%, 16.99%, and 17.31% of the BS accuracy loss due to mixed sliding-rolling motion, respectively. In addition, the average values of the absolute errors were changed from 0.0238 μm, 0.0505 μm, and 0.0589 μm to 0.0298 μm, 0.0549 μm, and 0.0665 μm. And the maximum values of the relative errors were decreased from 33.34%, 31.77%, and 33.66% to 10.64%, 14.07%, and 12.06%, and the average values of the relative errors were decreased from 11.18%, 11.19%, and 11.22% to 7.27%, 6.11%, and 6.67%.

3. According to accuracy decay analysis under AL + FR, the accuracy degradation due to rolling motion between the ball and raceway accounted for 18.16%, 18.58%, and 19.21% of the BS accuracy loss due to sliding motion, respectively. And the accuracy degradation due to rolling

motion between the ball and raceway accounted for 15.37%, 15.67%, and 16.11% of the BS accuracy loss due to mixed sliding-rolling motion. And the maximum values of the relative errors were reduced from 35.29%, 33.34%, and 38.36% to 16.17%, 14.26%, and 14.30%, and the average values of the relative errors were reduced from 11.18%, 11.19%, and 11.22% to 8.50%, 7.05%, and 6.75%, respectively.

Author contribution Baobao Qi and Jiajia Zhao are responsible for providing overall research ideas. Chuanhai Chen, Xianchun Song, and Hongkui Jiang are responsible for the measurement of machine tool error data. Baobao Qi and Chuanhai Chen are responsible for experimental data analysis.

Funding This research was supported by the National Natural Science Foundation of China (grant no. 51975019, grant no. 51975012, grant no. 51905334), National Science and Technology Major Project (Key Processing Equipment for Large and Medium CNC in the Machine Tool Industry, grant no. TC210H035-009), and Shanghai Sailing Program (19YF1418600).

Availability of data and materials Not applicable.

Declarations

Ethics approval Not applicable.

Consent to participate Not applicable.

Consent for publication Not applicable.

Conflict of interest The authors declare no competing interests.

References

1. Wei CC, Lin JF (2003) Kinematic analysis of the ball screw mechanism considering variable contact angles and elastic deformations. J Mech Des 125(4):717–733
2. Chen CL, Jang MJ, Lin KC (2004) Modeling and high-precision control of a ball-screw-driven stage. Precis Eng 28(4):483–495
3. Wei CC, Lai RS (2011) Kinematical analyses and transmission efficiency of a preloaded ball screw operating at high rotational speeds. Mech Mach Theory 46(7):880–898
4. Zhou CG, Feng HT, Chen ZT, Ou Y (2016) Correlation between preload and no-load drag torque of ball screws. Int J Mach Tools Manuf 102:35–40
5. Gnanamoorthy R, Govindaraian N, Mutoh Y (2004) Effect of slid-roll ratio on the contact fatigue behavior of sintered and hardened steels. J Fail Anal Prev 4(2):78–83
6. Archard JF (1953) Contact and rubbing of flat surfaces. J Appl Phys 24(8):981–988
7. Wei CC, Liou WL, Lai RS (2012) Wear analysis of the offset type preloaded ball-screw operating at high speed. Wear 292:111–123
8. Xu GY, Tao WJ, Feng HT (2013) Model of precision loss for the precision ball screw. Adv Mater Res 753–755:1680–1685
9. Xu XH, Wang YH, Xu D (2014) Wear prediction of ball screw based on adhesive wear. Appl Mech Mater 635–637:261–265
10. Zhou CG, Ou Y, Feng HT, Chen ZT (2017) Investigation of the precision loss for ball screw raceway based on the modified Archard theory. Ind Lubr Tribol 69(2):166–173
11. Zhou CG, Zhou HX, Feng HT (2020) Experimental analysis of the wear coefficient of double-nut ball screws. Wear 446–447:203–214
12. Luo J, Dornfeld DA (2001) Material removal mechanism in chemical mechanical polishing: theory and modeling. IEEE Trans Semicond Manuf 14(2):112–133
13. Horng HJ (1998) An elliptic elastic-plastic asperity microcontact model for rough surfaces. J Tribol 120(1):82–88
14. Zhao JJ, Lin MX, Song XC, Zhao YF, Wei N (2020) A novel approach to predict the precision sustainability of ball screw under multidirectional load states. Proc IME C J Mech Eng Sci 235(7):1277–1296
15. Zhao JJ, Lin MX, Song XC, Guo QZ (2020) Analysis of the precision sustainability of the preload double-nut ball screw with consideration of the raceway wear. Proceedings of the Institution of Mechanical Engineers Part J-Journal of Engineering Tribology 234(9):1530–1546
16. Liu JL, Ma C, Wang S (2019) Precision loss modeling method of ball screw pair. Mech Syst Signal Process 136(1):106397
17. Wang K, Feng HT, Zhou CG, Ou Y (2021) Optimization measurement for the ball screw raceway profile based on optical measuring system. Meas Sci Technol 32(3):035010
18. Zhao JJ, Lin MX, Song XC (2021) A modeling method for predicting the precision loss of the preload double-nut ball screw induced by raceway wear based on fractal theory. Wear 486:204065
19. Telliskivi T (2004) Simulation of wear in a rolling–sliding contact by a semi-Winkler model and the Archard's wear law. Wear 256(7–8):817–831
20. Xu NN, Tang WC, Chen YJ, Bao DF, Guo Y (2015) Modeling analysis and experimental study for the friction of a ball screw. Mech Mach Theory 87:57–69
21. Qi BB, Cheng Q, Li SL, Liu ZF, Yang CB (2021) Precision loss of ball screw mechanism under sliding-rolling mixed motion behavior. Journal of Central South University 28(5):1357–1376
22. Cheng Q, Qi BB, Liu ZF, Yang CB, Zheng JG (2021) Positioning accuracy degradation and lifetime prediction of the ball screw considering time-varying working conditions and feed modes. Proceedings of the Institution of Mechanical Engineers Part B-Journal of Engineering Manufacture 235(6–7):943–957
23. Cheng Q, Qi BB, Chu HY, Zhang ZL, Liu ZF, Zheng JG (2021) The analysis on the influence of mixed sliding-rolling motion mode to precision degradation of ball screw. Proceedings of the Institution of Mechanical Engineers Part C-Journal of Mechanical Engineering Science 203–210:1989–1996
24. Pullen J, Williamson JBP (1972) On the plastic contact of rough surfaces. Proc Math Phys Eng Sci 103(2):1038–1047
25. Williamson JBP, Harris JAG (1956) The influence of dust particles on the contact of solids. Proc Royal Society of London 237(1211):560–573
26. Cheng Q, Qi BB, Liu ZF, Zhang CX, Xue DY (2019) An accuracy degradation analysis of ball screw mechanism considering time-varying motion and loading working conditions. Mech Mach Theory 134:1–23
27. Hu W, Westerlund P, Hilber P, Chen CH, Yang ZJ (2022) A general model, estimation, and procedure for modeling recurrent failure process of high-voltage circuit breakers considering multivariate impacts. Reliab Eng Syst Saf 220:108276
28. Zhang ZL, Cheng Q, Qi BB, Tao ZQ (2021) A general approach for the machining quality evaluation of S-shaped specimen based on POS-SQP algorithm and Monte Carlo method. J Manuf Syst 60:553–568
29. Niu P, Cheng Q, Liu ZF, Chu HY (2021) A machining accuracy improvement approach for a horizontal machining center based on analysis of geometric error characteristics. Int J Adv Manuf Technol 112(9):2873–2887
30. Jin TT, Yan CL, Chen CH, Yang ZJ, Tian HL, Guo JY (2021) New domain adaptation method in shallow and deep layers of the CNN for bearing fault diagnosis under different working conditions. Int J Adv Manuf Technol 10:1–12

31. Sun JK, Sun ZZ, Chen CH, Yan CL, Jin TT, Zhong Y (2021) Group maintenance strategy of CNC machine tools considering three kinds of maintenance dependence and its optimization. Int J Adv Manuf Technol. https://doi.org/10.1007/s00170-021-07752-6
32. Guo SJ, Jiang GD, Mei XS (2017) Investigation of sensitivity analysis and compensation parameter optimization of geometric error for five-axis machine tool. Int J Adv Manuf Technol 93(9–12):3229–3243
33. Wu HR, Zheng HL, Li XX, Rong ML, Fan J, Meng XP (2020) Robust design method for optimizing the static accuracy of a vertical machining center. Int J Adv Manuf Technol 109(7–8):2009–2022
34. Niu P, Cheng Q, Liu ZF, Chu HY (2021) A machining accuracy improvement approach for a horizontal machining center based on analysis of geometric error characteristics. Int J Adv Manuf Technol 112(9–10):2873–2887
35. Zhang YZ, Zhang CX, Yan J, Yang CB, Liu ZF (2022) Rapid construction method of equipment model for discrete manufacturing digital twin workshop system. Robot Comput Integr Manuf 75:102309
36. Ding H, Kahraman A (2007) Interactions between nonlinear spur gear dynamics and surface wear. J Sound Vib 307(3/4/5): 662−679
37. Chen YJ, Tang WC (2014) Dynamic contact stiffness analysis of a double-nut ball screw based on a quasi-static method. Mech Mach Theory 73:76–90
38. Kalker JJ (1991) Wheel-rail rolling contact theory. Wear 144(1–2):243–261
39. Rodríguez-Tembleque L, Abascal R, Aliabadi MH (2010) A Boundary element formulation for wear modeling on 3d contact and rolling-contact problems. Int J Solids Struct 47(18):2600–2612
40. Chen K, Zu L, Wang L (2018) Prediction of preload attenuation of ball screw based on support vector machine. Adv Mech Eng 10(9):1–10